Published in final edited form as:
Stroke. 2009 March ; 40(3): 959–965. doi:10.1161/STROKEAHA.108.524124.

The Asymmetric Vascular Stent: Efficacy in a rabbit aneurysm model

Ciprian N Ionita, PhD, **Ann M Paciorek, MS**, **Andreea Dohatcu, BSc**, **Kenneth R Hoffmann, PhD**, **Daniel R Bednarek, PhD**, **John Kolega, PhD**, **Elad I Levy, MD**, **L. Nelson Hopkins, MD**, **Stephen Rudin, PhD**, and **J. Mocco, PhD**

Departments of Neurosurgery (CNI, AMP, KRH, EIL, LNH, SR, JM) and Radiology (CNI, DRB, EIL, LNH, SR) and Pathology (JK) & Physics(AD, KRH, DRB) and Toshiba Stroke Research Center (CNI, AMP,AD, KRH, DRB, EIL, LNH, SR), School of Medicine and Biomedical Sciences, University at Buffalo, State University of New York; Department of Neurosurgery (EIL, LNH, JM), Millard Fillmore Gates Hospital, Kaleida Health, Buffalo, New York

Abstract

Background and Purpose—Development of hemodynamic modifying devices to treat intracranial aneurysms (IAs) is an active area of research. The asymmetric vascular stent (AVS), a

Correspondence: Ciprian N Ionita BRB Bldg Rm 445 3435 Main St Buffalo, NY 14221 Tel: 716 829 3596 ext 121 Fax: 716 829 2212 Email: E-mail: cnionita@buffalo.edu.

Author Contributions

Guarantor of integrity of the entire study: S Rudin, C N Ionita
Study concepts: S. Rudin, C N Ionita
Study design: S. Rudin C N Ionita
Literature research: C N Ionita, J Mocco, A M Paciorek
Experimental studies: C N Ionita, A. Dohatcu, A M Paciorek
Data acquisition: C N Ionita, A. Dohatcu, A M Paciorek
Data interpretation: C N Ionita, J Mocco, S. Rudin, A M Paciorek, K R Hoffmann, D R Bednarek, J Kolega
Statistical analysis: C N Ionita, J Mocco, S Rudin, K R Hoffmann
Participated in discussion and guidance in the research: C N Ionita, S. Rudin, K R Hoffmann, D R Bednarek
Handled funding and supervision: S Rudin, D R Bednarek
Manuscript preparation: All authors
Critical review for intellectual content: All authors
Manuscript revision or review and final version approval: All authors

Conflicts on Interest Disclosures

- Dr. Ionita has received support from the grants named below.
- Ms. Paciorek has received support through the NIH grants named below.
- Ms. Dohatcu has received support through the NIH grants named below
- Dr. Hoffmann has nothing to disclose regarding potential financial conflicts of interest.
- Dr. Bednarek has received research support through a Toshiba equipment grant.
- Dr. Kolega serves as a consultant for/advisor to Boston Scientific.
- Dr. Levy has received industry grant support and honoraria from Boston Scientific Corporation and Cordis Corporation; and receives patent royalties from Zimmer Spine and remuneration from Abbott Vascular and eV3, Inc. for carotid stent training.
- Dr. Hopkins has received industry grant support from Boston Scientific Corporation, Cordis Corporation, and Micrus; is a stock- or shareholder in Boston Scientific Corporation, Micrus, AccesClosure and SquareOne Inc; receives consulting fees from Micrus, Boston Scientific Corporation, Abbott Laboratories, C. R. Bard, Inc., and Cordis Corporation; has received honoraria from C. R. Bard, Inc., Boston Scientific Corporation, Cordis Corporation
- Dr. Mocco has received a research grant from the Brain Aneurysm Foundation.
- Dr. Rudin is the principal investigator of the research grants named below and has received research support through a Toshiba equipment grant.

stent containing a low porosity patch, is such device. We evaluate AVS efficacy in an in vivo IA model.

Methods—We created twenty-four elastase rabbit model aneurysms: thirteen treated with the AVS, five treated with standard coronary stents, and six untreated controls. Four weeks following treatment, aneurysms underwent follow-up angiography, cone-beam micro-CT, histologic evaluation, and selective electron microscopy scanning.

Results—Four rabbits died early in the study: three during AVS treatment and one control (secondary to intra-procedural vessel injury and an unrelated tumor, respectively). AVS-treated aneurysms exhibited very weak or no aneurysm flow immediately after treatment and no flow in all aneurysms at follow-up. Stent-treated aneurysms showed flow both after treatment (5/5) and at follow-up (3/5). All control aneurysms remained patent during the study. Micro-CT scans showed: 9/9 of scanned AVS aneurysms were occluded, (6/9) AVSs were ideally placed and (3/9) the low porosity region partially covered the aneurysm neck; stent-treated aneurysms were 1/5 occluded, 2/5 patent, and 2/5 partially-patent. Histology results demonstrated: for AVS-treated aneurysms, advanced thrombus organization in the (9/9); for stent-treated aneurysms (1/4) no thrombus, (2/4) partially-thrombosed and (1/4) fully-thrombosed; for control aneurysms (4/4) no thrombus.

Conclusion—The use of AVSs shows promise as a viable new therapeutic in intracranial aneurysm treatment. These data encourage further investigation and provide substantial support to the AVS concept.

Keywords

Asymmetric Vascular Stent; elastase aneurysm model; hemodynamics modification

Introduction

Intracranial aneurysm (IA) treatment using flow alteration induced by stents is a subject studied intensely by a number of endovascular research groups.[1-18] The primary hypothesis is that flow diversion can induce intra-aneurysmal thrombus formation thereby resulting in aneurysm exclusion from the circulation.[19] The goal is to achieve aneurysm exclusion while maintaining a low probability of perforator occlusion[19], in-stent restenosis, thromboembolic events or vessel injury. Potential benefits of such a treatment would include: reduced procedure time, lower dome perforation risk, shorter recovery time, reduced aneurysm recanalization, and reduced costs.

Various groups have reported both in-vitro and in-vivo results of aneurysm treatment with commercially available stents. [1, 7-10, 13] However, stent-only treatment did not attain the desired reproducibility of IA occlusion. [2, 7, 8] Aneurysm dome hemodynamics are very different from one case to another as indicated by computational fluid dynamics analysis of patient-specific aneurysm geometries.[1] As a result, current commercially available stents do not provide sufficient flow diversion to consistently alter significantly intra-aneurysmal flow.

We developed a novel stent, called an Asymmetric Vascular Stent (AVS) that is extremely low porosity in a relatively small, specific portion of the stent. [3-5, 11, 14] The device was built by adding a fine low-porosity stainless steel mesh onto an existing standard high-porosity stent structure. Ideally the device is deployed so the dense patch covers the aneurysm neck. Intra-aneurysmal flow alterations with the new device have been studied extensively with phantoms[4, 14] or using computational fluid dynamics.[3, 11] Phantom studies[4] using particle image velocimetry indicated radical flow changes with AVS-treated aneurysms compared to traditional stent designs. We reported two orders of magnitude decrease in the velocity and vorticity, and reduced aneurysmal wall shear stress. Additionally, in-vitro angiographic studies

using the AVS[14, 18] demonstrated drastic reduction of iodine contrast in the aneurysm dome and prolonged contrast presence following injection, signifying decreased flow within the aneurysm.

Preliminary AVS in-vivo verification was done in a small pilot study [5] using canine aneurysms model. The study indicated that the treatment method is possible, the aneurysms treated with the AVS demonstrated thrombosis and the complications were minimal. However, before further efforts can be made to translate the AVS into a viable therapy in humans, its efficacy in-vivo must be demonstrated in multiple models, including those with vessel sizes more comparable to human intracranial vessels. Therefore, we present an in-vivo efficacy study performed in a rabbit aneurysm model.[20]

Material and Methods

Aneurysm creation

All procedures were approved by the Institutional Animal Care and Use Committee of the State University of New York at Buffalo and were conducted according to guidelines established by the animal welfare act. Twenty-four New Zealand White rabbits (7.5 ± .75 kg; 6−8 kg; mean ± STD, range) underwent right carotid aneurysm creation using previously described techniques[7, 8, 20]. Following three weeks of aneurysm maturation, the subjects underwent angiographic evaluation and treatment. The subjects were divided into three cohorts: those treated with AVS (n=13), those treated with standard coronary stents (Guidant Corp. Santa Clara, CA) (n=5), and those undergoing no treatment (n=6).

AVS stent prototype description and stent deployment procedure

The AVS (Figure 1) is built by laser micro-welding a low-porosity stainless steel 316 L cloth mesh (50 μm thick and 500 wires/inch) onto a standard balloon-expandable coronary stent (Multi-link Vision, Guidant Corp. Santa Clara, CA.). We thus used the same stainless steel alloy for the mesh as that used in the fabrication of coronary stents, in order to ensure the use of a material with well documented thrombogenicity profile.[21] The porosity, defined as the percent of open area within the total mesh area, is 25%. The fine stainless steel mesh structure allows stent crimping onto a balloon-tipped catheter and subsequent expansion without structural device damage.

Once crimped, AVSs have average diameter of 1.3 mm. The patch shape was patterned to fit typical side-wall aneurysm geometry, and therefore was laser-cut in an ellipse with a short axis between 5 and 6 mm and a long axis between 6 and 8 mm. Stent and patch diameters were chosen based on measurements from 3D aneurysm renderings derived from a rotational DSA system, and from published literature.[8] For each subject, 4 different patch size AVSs were available for treatment. Stent positioning and deployment were performed under direct fluoroscopic guidance. Platinum markers label the patch quadrants to unambiguously indicate the stent orientation (Figure 1)[22], thereby allowing rotational placement accuracy of better than 12 degrees when a 5-inch image intensifier is used.

Animals received heparin 1000 units intra-procedurally. A 6 Fr. Terumo Pinnacle sheath (Boston Scientific, Mountain View, CA) was introduced into the left femoral artery, and a 6 Fr. Envoy guiding straight-tip catheter (Cordis Endovascular Systems, Miami, FL) was advanced under road-mapped fluoroscopic guidance to the innominate artery. A 3D rendered image based on rotational DSA (Vital Images, Minnetonka, MN) was used to guide selection of a C-arm orientation that best visualized the aneurysm neck while remaining orthogonal to the parent vessel's long axis. The AVS was then advanced over a Synchro-14 guide wire (Boston Scientific, Mountain View, CA) under roadmap guidance and positioned so the

proximal and distal platinum markers were adjacent to and spanned the entirety of the aneurysm neck, while the middle platinum markers were overlapping (Figure 1). The stent-delivery balloon was then inflated.

Angiographic analysis

Angiographic data was acquired pre-procedure, immediately post-procedure (after stent deployment), and at four weeks follow-up. Contrast inflow was graded on a three tiered scale: Fast (F), Slow (S), and Occluded (O). Fast flow is characterized by a rapid aneurysm opacification with likewise relatively quick contrast clearance - less than 5 seconds. The contrast is observed to enter the aneurysms as a small focused jet. Slow (S) flow, enters the aneurysm in a more cloud-like dispersion and remains opacified for greater than 5 seconds. Occluded (O), is characterized by zero contrast entering the aneurysm.

Contrast pooling, another monitored aspect, occurs when gravitational forces acting on the contrast are stronger than the hemodynamic ones. This unbalance causes the contrast to settle in the aneurysm for a very long time, more than a minute in some cases. Previous work[24] indicates contrast pooling as a very strong indication of slow flow in certain areas of the aneurysms.

Cone-beam micro-CT analysis

After 4 weeks follow-up, aneurysms were fixed by pressure perfusion at time of sacrifice using 0.9% neutral buffered formalin, then explanted and stored in the same solution at 4°C for 48 hours for further analysis. 19 of 20 samples were scanned using cone beam micro-CT. The cone-beam micro-CT[23] scanner consists of a micro-focal spot x-ray tube, a rotary stage, and a micro-angiographic detector with a 45 microns pixel size. Aneurysm samples were connected to an air-flow circuit for 1−3 minutes to remove as much of the neutral buffered formalin solution as possible. In this way air was used as contrast agent in order to visualize the vessel lumen and the potentially untreated portions of the aneurysms.

Histological analysis

For histological evaluation, aneurysm domes were excised from the parent vessel, processed, embedded in paraffin, and cut in 2 μm thick slices taken from the midpoint of the aneurysm in the coronal orientation (same direction as the parent artery) using a rotary microtome (Microm International, HM355S, Kalamazoo, MI). Slides were stained with Hematoxylin and Eosin (H&E) for overall structural analysis and Masson Tri-Chrome for determination of collagen deposition. Unlike the angiographic and micro-CT evaluations wherein stent visualization prevented appropriate blinding, microscopic analysis was performed by two observers in a blinded fashion. A grading scale was used to evaluate the occurrence of aneurysm dome and neck organized thrombus: 0 (zero) for less than 2% thrombus; 1 (one) for 2% to 10% thrombus; 2 (two) for 10% to 50%, 3 (three) for 50% to 90% and 4 (four) if more than 90% of the area was filled with organized thrombus.

Scanning Electron Microscopy (SEM)

SEM was performed on one specific AVS-stented artery specimen. This specimen was fixed using isotonic 2.5% gluteraldahyde in 0.1M sodium cacodylate (Polysciences, Warrington, PA). The arterial trunk was longitudinally cut, opposite the aneurysm neck and the vessel walls were opened, and SEM of the parent vessel performed for an “in-vessel” view of the surface covering the stent and the stent patch. The samples were washed in distilled water, dehydrated in ethanol (70%−100%), dried with hexamethyldisilazane (HMDS) (Polysciences, Warrington, PA), and stored overnight in a desiccator. SEM was performed using a field

emission scanning electron microscope (Hitachi #9000, Schaumburg, IL) in high vacuum mode.

Statistical Analysis

Data is presented as mean±SD; (range). Statistical analysis was performed using GraphPad InStat (GraphPad Software Inc. San Diego, CA). Student's t-tests assuming equal variances were used to determine statistical significance of aneurysm geometry and aneurysm histology. Fisher's Exact test was used for angiographic categorical results. Significance was defined as $p<0.05$.

Results

Aneurysm Creation

Aneurysmal geometries, were: vessel size = 4.47±029; (4.07, 5.12) mm; aneurysm neck = 3.32 ±0.75; (2.11, 4.69) mm; aneurysmal dome size =5.79±2.83; (2.63, 12); dome to neck ratio = 1.80±0.84; (0.88, 2.78). There were no statistically significant differences among the three experimental cohorts.

Procedural results

24 rabbits were divided in three groups: AVS-treated (13/24), Stent-treated (5/24) and (6/24) Control. Relevant procedure was successful in (10/13) AVS, (5/5) Stent and (6/6) Control. Vessel injury prior to stent deployment occurred in three AVS animals that were sacrificed as required by IACUC protocol. Each of these sacrifices occurred early in the study (3 of the first 4 animals) and was the result of vessel perforation during AVS positioning (one superficial cervical artery and two axillary artery injuries). Once appropriate techniques were learned, zero of the final 9 animals suffered perforation.

Follow-up was done on the successfully-treated subject (10/10) AVS, (5/5) Stent and (5/6) control. 1/6 Control developed a mammary gland tumor and was excluded. CB Micro-CT (μ-CT) was done in (9/10) AVS, (5/5) Stent and (5/5) Control. 1/10 AVS sample was used (SEM) which excluded the Micro-CT analysis. All 20 samples explanted at follow up underwent preparation for dome and neck histology analysis. During the embedding and cutting some samples were severely damaged or affected by artifacts and were not graded. The neck was graded in 8/10 AVS, 3/5 stent and 4/5 control. The dome was graded in 9/10 AVS, 4/5 stent and 4/5 for controls.

For the AVS cohort, aneurysm neck coverage was complete in (7/10) and only partial in (3/10). Neck partial coverage was: 50 % for #16, 75% for #17 and more than 90% for #18.

Angiographic Analysis Results

Angiographic results are summarized in Table 1. (18/20) surviving animals' aneurysms (90%) showed strong initial aneurysm contrast flow, while (2/10) showed slow contrast followed by pooling: #6 (stent cohort) and #11(AVS cohort). Immediately after traditional stent-treatment, two aneurysms (40%) showed fast contrast diffusion, two (40%) showed slow perfusion (#8, #10) and one (20%) was fully occluded (#9). Immediately following AVS treatment nine aneurysms (90%) were completely obliterated while one (10%) showed slow perfusion (#17).

At 28 days follow-up, AVS-treated aneurysms resulted in more consistent aneurysm occlusion compared to treatment with traditional stents ($p<0.01$) or no treatment ($p<0.01$). All five control aneurysms were patent. Two of the stent-treated aneurysms (40 %) had fast flow (#8, #10), two had slow perfusion (#6. #7) and one was occluded (#9). All AVS-treated aneurysms were occluded.

Cone Beam Micro-CT Results

The CB micro-CT scanner was used to evaluate the stent placement with respect to the aneurysm neck and thrombus formation. Central CT slices taken across the vessel and the aneurysm domes are shown in Figure 2 for one case each: untreated, treated with a stent, and treated with an AVS.

CT scans of the five untreated animals showed patent aneurysm domes, with no sign of thrombosis. Two stent-treated aneurysms (#8, #10) were patent with no sign of thrombus formation, two others had remnant necks (#6, #7), and one was fully thrombosed (#9). All AVS-treated aneurysms were occluded.

Histology Results

Histology results are summarized in Table 1, and Figure 4 (left section). Four aneurysms from the control cohort successfully underwent histological analysis. None of the control aneurysm necks contained thrombus, however, (2/4) had some thrombus in the dome; 1 had approximately 4% organized thrombus and 1 contained 2−4% un-organized clot.

(4/5) stent-treated aneurysms underwent histology analysis; one demonstrated severe cutting artifacts and could not be graded. All four remaining aneurysm domes had thrombus; two contained 10%−50% organized thrombus, one with >50% organized thrombus, and one filled with only organized thrombus.

(9/9) AVS-treated aneurysms that underwent histological analysis contained organized thrombus in both the neck and in the dome; of these, 8 had greater than 50% organized thrombus in the dome with organized tissue spanning the neck.

At 28 days follow-up, AVS-treated aneurysms neck histology showed more organized thrombus compared to treatment with traditional stents or no treatment. T-test analysis indicate better neck occlusion for the AVS than the regular stents with a large statistical significance (1.3±2, 3.88±0.35; $p=0.004$). Results for dome filling with organized thrombus for Stent versus AVS samples was (2.5±1.29, 3.11±0.78, $p>0.05$). All five control aneurysm necks were patent.

Scanning Electron Microscopy Results

After initial processing for SEM, low-magnification light microscopic inspection (5x) of the stented aneurysm and neck region revealed new tissue growth within the patched aneurysm neck and on some large stent struts (Figure 3). The entire fine mesh patch was covered with a shiny layer consistent with endothelialization. Details obtained with the electron microscope are shown in Figure 3. While this SEM analysis demonstrated new intima growth over the stent struts, stent mesh and aneurysm neck, we cannot extrapolate that this occurred in all other cases given there was only one specimen analyzed with SEM.

Discussion

We demonstrate in-vivo efficacy of a new AVS designed for the sidewall intracranial aneurysm (IA) treatment. Ten aneurysms were successfully treated. AVS-treated aneurysms resulted in more consistent aneurysm occlusion compared to treatment with traditional stents or no treatment.

All aneurysms occluded post-treatment remained occluded at follow-up. Immediately following deployment occlusion was observed in 90% of the AVS-treated aneurysms and in only one (20%) of the stent group. Interestingly, while the one AVS that demonstrated slow flow immediately following deployment went on to total occlusion, both of the two stent-

treated animals that showed changes from Fast (F) to Slow (S) flow immediately following treatment demonstrated a return of fast flow at the four week follow-up. As the use of stent assisted coiling has become increasingly utilized over the past five years, it has become evident that current, traditional stents do not consistently lead to IA thrombosis and recanalization remains a significant problem.[25-31] This promising initial data suggests that the use of an AVS-type device may substantially increase IA occlusion rates while decreasing recanalization rates.

All surviving AVS-treated animals had complete aneurysm occlusion at the 28 day follow-up regardless of the percent aneurysms neck coverage measured after micro-CT scanning. These results compare favorably to recent endoluminal flow disruption device iterature.[6] It should also be noted that at least 50% of aneurysm neck coverage was achieved in all cases. We find it encouraging that such a high rate of successful occlusion can be achieved with only a portion of the stent being low porosity and anticipate continued success with improving AVS designs. However, caution must be expressed as the current AVS iteration has substantial mechanical limitations.

First, while AVS placement was ideal in 66% of the nine micro-CT scanned AVS-treated aneurysms, balloon rotation during inflation caused slight miss-placement of three stents. It is likely that such technical difficulties will be alleviated once a self-expanding stent is used as the base structure rather than a balloon-mounted stent - thereby removing the substantial rotation component associated with balloon-mounted stent deployment. It should be noted though, that despite partial-neck coverage the hemodynamics were modified sufficiently to cause full IA thrombosis in all aneurysms at the four week follow-up.

Second, the AVS prototype described herein cannot likely be used in its current configuration for the more tortuous vasculature approach encountered in human neurovascular anatomy. The fine stainless mesh patch adds stiffness to the already fairly rigid balloon expandable device. Our three point flexure rigidity measurements show a 15−20% increase in the AVS's stiffness compared to the bare stent. In any case these data provide important proof of concept in a small animal model and are an important step in the translation of this technology towards clinical application. Current commercially available self-expanding stents that are specifically designed for intracranial use have greatly improved navigability compared to the previously used balloon mounted coronary stents and as a result have greatly increased the number of lesions treatable by endovascular means. [25-31]

Three deaths occurred in the AVS cohort. All three were within the first four AVS treatment experiments and were secondary to vessel injury during AVS alignment. As accurate localization of the aneurysm neck is essential for AVS treatment, we would advance the AVS distal to the aneurysm neck during roadmap acquisition - thereby avoiding the roadmap miss-registration. These vessel injuries occurred while advancing the AVS past the aneurysms location. One injury was secondary to AVS advancement into the superficial cervical artery and two were secondary to AVS advancement into the axillary artery. These complications were eliminated once we were aware of the potential injury and careful attention was paid to the distal vasculature, and by using AVSs no longer than 15mm. The clear value of this learning curve is evidenced by the fact that none of the remaining nine animals suffered this complication.

A potential complication of endoluminal flow disruption is perforator occlusion. While we experienced no occurrence of nearby vessel thrombosis, the current model does not allow adequate assessment of this potential complication due to the lack of small vessel origins in the vicinity of the aneurysm. Data exist documenting excellent perforator patency maintenance with stents of approximately 70% porosity [6, 32], well below the 80% porosity of the majority

of the AVS. We are currently working to assess the risk of perforator occlusion resulting from low porosity mesh coverage of vessel ostia.

The current study shows treatment of sidewall aneurysms only, however we are currently endeavoring to develop self-expanding AVS alternatives with substantially improved flexibility and navigability and we anticipate that such a re-tooling will also lead to improved applicability of this technology. To increase flexibility, in recent preliminary studies [33, 34] we replaced the stainless steel patch with a polyurethane membrane (ChronoFlex AR, Cardiotech International Inc.). We simulated treatment in patient specific side-wall[33] and basilar-tip[34] aneurysm phantoms using the AVS as a flow diverter. The optical flow study revealed significant flow reduction in the aneurysms, with partial aneurysm orifice blockage. Extension of the current latest AVS fabrication to self expending stents is expected in the future.

Conclusion

We demonstrate a high degree of efficacy utilizing a new endoluminal flow diverter, the AVS, to treat aneurysms in a rabbit elastase aneurysm model. Following AVS treatment, 100% of aneurysms were occluded at the four week follow-up. Complications were encountered early in the series but, once identified, were completely avoidable in the latter portion of the study. These data support the development and likely eventual potential benefit of AVS technology in sidewall aneurysm treatment. However, substantial improvements in stent flexibility and deployment methods are likely necessary before translation to humans can be achieved.

Acknowledgments

We thank Peter Bush for expertise and equipment used in the Scanning Electron Microscopy evaluations, Guidant Corp. for the stents used in this study and Toshiba Medical Systems Corp. for x-ray imaging equipment.

Funding for this Study

Supported in part by NIH Grants R01NS43924 and R01EB002873.

References

1. Cebral JR, Castro MA, Burgess JE, Pergolizzi RS, Sheridan MJ, Putman CM. Characterization of cerebral aneurysms for assessing risk of rupture by using patient-specific computational hemodynamics models. American Journal of Neuroradiology 2005;26:2550–2559. [PubMed: 16286400]
2. Doerfler A, Wanke I, Egelhof T, Stolke D, Forsting M. Double-stent method: Therapeutic alternative for small wide-necked aneurysms. Journal of Neurosurgery 2004;100:150–154. [PubMed: 14743929]
3. Hoi Y, Ionita CN, Tranquebar RV, Hoffmann KR, Woodward SH, Taulbee DB, Meng H, Rudin S. Flow modification in canine intracranial aneurysm model by an asymmetric stent: Studies using digital subtraction angiography (DSA) and image-based computational fluid dynamics (cfd) analyses. Proc SPIE 2006;6143:61430J.
4. Ionita CN, Hoi Y, Meng H, Rudin S. Particle image velocimetry (piv) evaluation of flow modification in aneurysm phantoms using asymmetric stents. Proc SPIE 2004;5369:295–306.
5. Ionita CN, Paciorecк A, Hoffmann KR, Bednarek DR, Yamamoto J, Kolega J, Levy EI, Hopkins LN, Rudin S, Mocco J. Asymmetric vascular stent (avs):Feasibility study of a new low-porosity patch-containing stent. Stroke. 2008in print
6. Kallmes DF, Ding YH, Dai D, Kadirvel R, Lewis DA, Cloft HJ. A new endoluminal, flow-disrupting device for treatment of saccular aneurysms. Stroke 2007;38:2346–2352. [PubMed: 17615366]
7. Krings T, Busch C, Sellhaus B, Drexler AY, Bovi M, Hermanns-Sachweh B, Scherer K, Gilsbach JM, Thron A, Hans FJ. Long-term histological and scanning electron microscopy results of endovascular and operative treatments of experimentally induced aneurysms in the rabbit. Neurosurgery 2006;59:911–923. [PubMed: 17038956]discussion 923−914

8. Krings T, Hans FJ, Moller-Hartmann W, Brunn A, Thiex R, Schmitz-Rode T, Verken P, Scherer K, Dreeskamp H, Stein KP, Gilsbach JM, Thron A. Treatment of experimentally induced aneurysms with stents. Neurosurgery 2005;56:1347–1359. [PubMed: 15918952]
9. Lieber BB, Gounis MJ. The physics of endoluminal stenting in the treatment of cerebrovascular aneurysms. Neurological Research 2002;24:S33–S42. [PubMed: 12074435]
10. Lieber BB, Livescu V, Hopkins LN, Wakhloo AK. Particle image velocimetry assessment of stent design influence on intra-aneurysmal flow. Annals of Biomedical Engineering 2002;30:768–777. [PubMed: 12220077]
11. Minsuok K, Ciprian I, Rekha T, Kenneth RH, Dale BT, Hui M, Stephen R. Evaluation of an asymmetric stent patch design for a patient specific intracranial aneurysm using computational fluid dynamic (CFD) calculations in the computed tomography (CT) derived lumen 2006;6143:61432G.
12. Rhee K, Han MH, Cha SH. Changes of flow characteristics by stenting in aneurysm models: Influence of aneurysm geometry and stent porosity. Annals of Biomedical Engineering 2002;30:894–904. [PubMed: 12398420]
13. Roy D, Milot G, Raymond J. Endovascular treatment of unruptured aneurysms. Stroke 2001;32:1998–2004. [PubMed: 11546888]
14. Rudin S, Wang Z, Kyprianou I, Hoffmann KR, Wu Y, Meng H, Guterman LR, Nemes B, Bednarek DR, Dmochowski J, Hopkins LN. Measurement of flow modification in phantom aneurysm model: Comparison of coils and a longitudinally and axially asymmetric stent - initial findings. Radiology 2004;231:272–276. [PubMed: 15068953]
15. Sadasivan C, Lieber BB, Gounis MJ, Lopes DK, Hopkins LN. Angiographic quantification of contrast medium washout from cerebral aneurysms after stent placement. American Journal of Neuroradiology 2002;23:1214–1221. [PubMed: 12169482]
16. Tenjin H, Asakura F, Nakahara Y, Matsumoto K, Matsuo T, Urano F, Ueda S. Evaluation of intraaneurysmal blood velocity by time-density curve analysis and digital subtraction angiography. American Journal of Neuroradiology 1998;19:1303–1307. [PubMed: 9726473]
17. Wakhloo AK, Lanzino G, Lieber BB, Hopkins LN. Stents for intracranial aneurysms: The beginning of a new endovascular era? Neurosurgery 1998;43:377–379. [PubMed: 9696095]
18. Wang Z, Ionita CN, Rudin S, Hoffmann KR, Paxton AB, Bednarek DR. Angiographic analysis of blood flow modification in cerebral aneurysm models with a new asymmetric stent. Proc SPIE 2004;5369:307–318.
19. Wootton DM, Ku DN. Fluid mechanics of vascular systems, diseases, and thrombosis. Annual Review of Biomedical Engineering 1999;1:299–329.
20. Altes TA, Cloft HJ, Short JG, DeGast A, Do HM, Helm GA, Kallmes DF. Creation of saccular aneurysms in the rabbit: A model suitable for testing endovascular devices. American Journal of Roentgenology 2000;174:349–354. [PubMed: 10658703]
21. Bertrand OF, Sipehia R, Mongrain R, Rodes J, Tardif J-C, Bilodeau L, Cote G, Bourassa MG. Biocompatibility aspects of new stent technology. J Am Coll Cardiol 1998;32:562–571. [PubMed: 9741494]
22. Ionita CN, Rudin S, Hoffmann KR, Bednarek DR. Microangiographic image-guided localization of a new asymmetric stent for treatment of cerebral aneurysms. Proc SPIE 2005;5744:354–365.
23. Wang ZJ, Hoffmann KR, Wang Z, Rudin S, Guterman LR, Meng H. Contrast settling in cerebral aneurysm angiography. Physics in Medicine and Biology 2005;50:3171–3181. [PubMed: 15972988]
24. Ionita CN, Hoffmann KR, Bednarek DR, Chityala R, Rudin S. Cone-beam micro-ct system based on labview software. J Digit Imaging. 2007
25. Akpek S, Arat A, Morsi H, Klucznick RP, Strother CM, Mawad ME. Self-expandable stent-assisted coiling of wide-necked intracranial aneurysms: A single-center experience. American Journal of Neuroradiology 2005;26:1223–1231. [PubMed: 15891189]
26. Benitez RP, Silva MT, Klem J, Veznedaroglu E, Rosenwasser RH. Endovascular occlusion of wide-necked aneurysms with a new intracranial microstent (Neuroform) and detachable coils. Neurosurgery 2004;54:1359–1367. [PubMed: 15157292]
27. Biondi A, Janardhan V, Katz JM, Salvaggio K, Riina HA, Gobin YP. Neuroform stent-assisted coil embolization of wide-neck intracranial aneurysms: Strategies in stent deployment and midterm follow-up. Neurosurgery 2007;61:460–468. [PubMed: 17881956]

28. Fiorella D, Albuquerque FC, Deshmukh VR, McDougall CG. Usefulness of the Neuroform stent for the treatment of cerebral aneurysms: Results at initial (3−6-mo) follow-up. Neurosurgery 2005;56:1191–1201. [PubMed: 15918935]

29. Fiorella D, Albuquerque FC, Han P, McDougall CG. Preliminary experience using the neuroform stent for the treatment of cerebral aneurysms. Neurosurgery 2004;54:6–16. [PubMed: 14683536]

30. Lylyk P, Ferrario A, Pabon B, Miranda C, Doroszuk G. Buenos aires experience with the neuroform self-expanding stent for the treatment of intracranial aneurysms. Journal of Neurosurgery 2005;102:235–241. [PubMed: 15739550]

31. Weber W, Bendszus M, Kis B, Boulanger T, Solymosi L, Kuhne D. A new self-expanding nitinol stent (enterprise) for the treatment of wide-necked intracranial aneurysms: Initial clinical and angiographic results in 31 aneurysms. Neuroradiology 2007;49:555–561. [PubMed: 17476494]

32. Lopes DK, Ringer AJ, Boulos AS, Qureshi AI, Lieber BB, Guterman LR, Hopkins LN. Fate of branch arteries after intracranial stenting. Neurosurgery 2003;52:1275–1278. [PubMed: 12762872]

33. Dohatcu AC, Ionita CN, Sherman R, Rangwalla HS, Bednarek DR, Hoffman KR, Rudin S. Regional Time Density Curves (R-TDC) derived from angiographic sequences for analysis of aneurysmal flow modification resulting from endovascular Image-Guided Interventions. Med. Phys 2007;34:2367.

34. Sherman JR, Rangwala HS, Ionita CN, Dohatcu AC, Lee JW, Bednarek DR, Hoffmann KR, Rudin S. Investigation of new flow modifying endovascular image-guided interventional (EIGI) techniques in patient-specific aneurysm phantoms (PSAPs) using optical imaging. Proc SPIE 2008;6918:69181V-1–69181V-11.

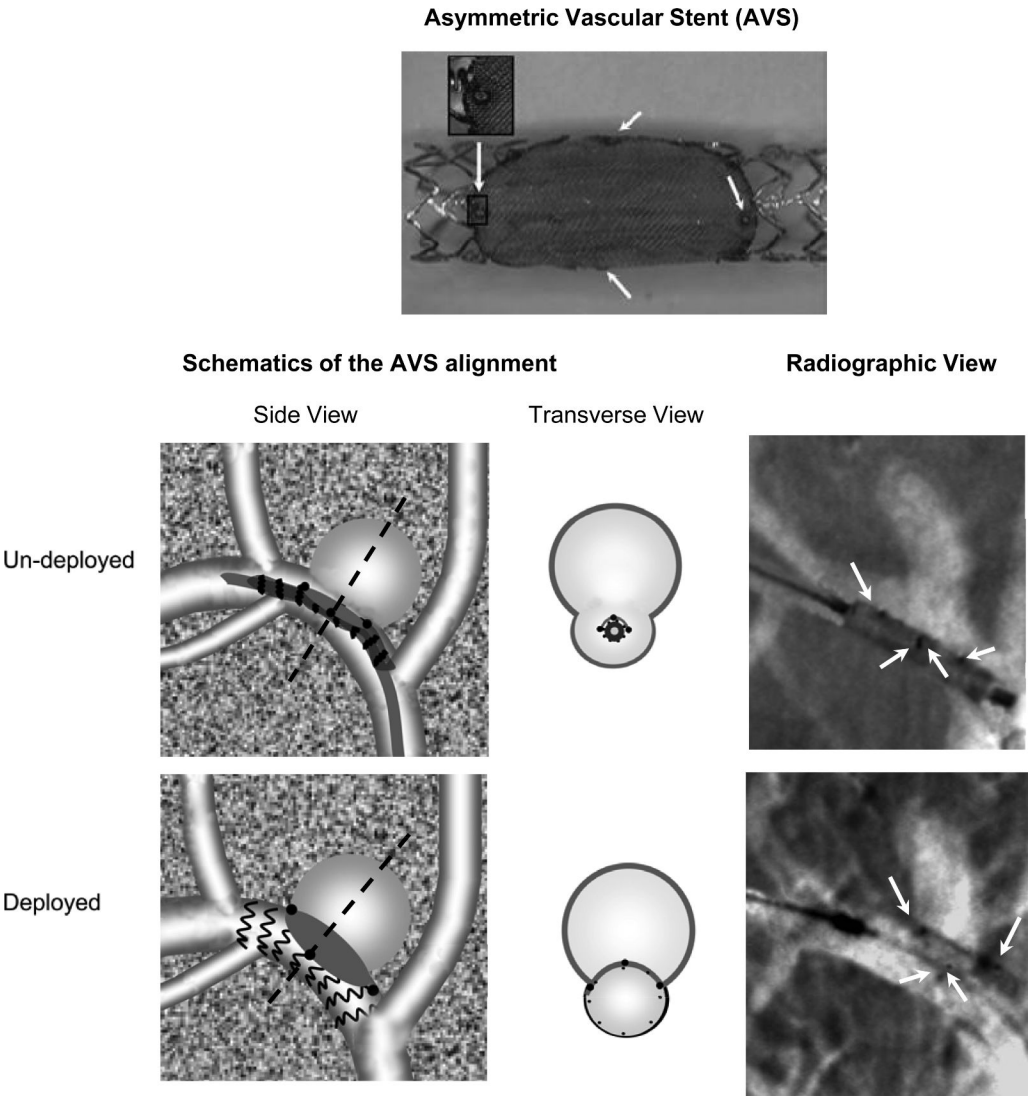

Figure 1.
Example of an Asymmetric Vascular Stent (AVS) (top), stenting procedure schematics and radiographic snapshots. For the AVS (top) the gray area is the fine mesh and the arrows indicate the platinum markers micro-welded at the ends of the patch. The schematics of the alignment are shown on the bottom left. The Side View shows the projection image corresponding to the Radiographic View while the Transverse View shows a cut perpendicular on the projection plane passing through the dotted line. In the radiographic images taken before and after the deployment, the white arrows indicate the positions of the AVS markers.

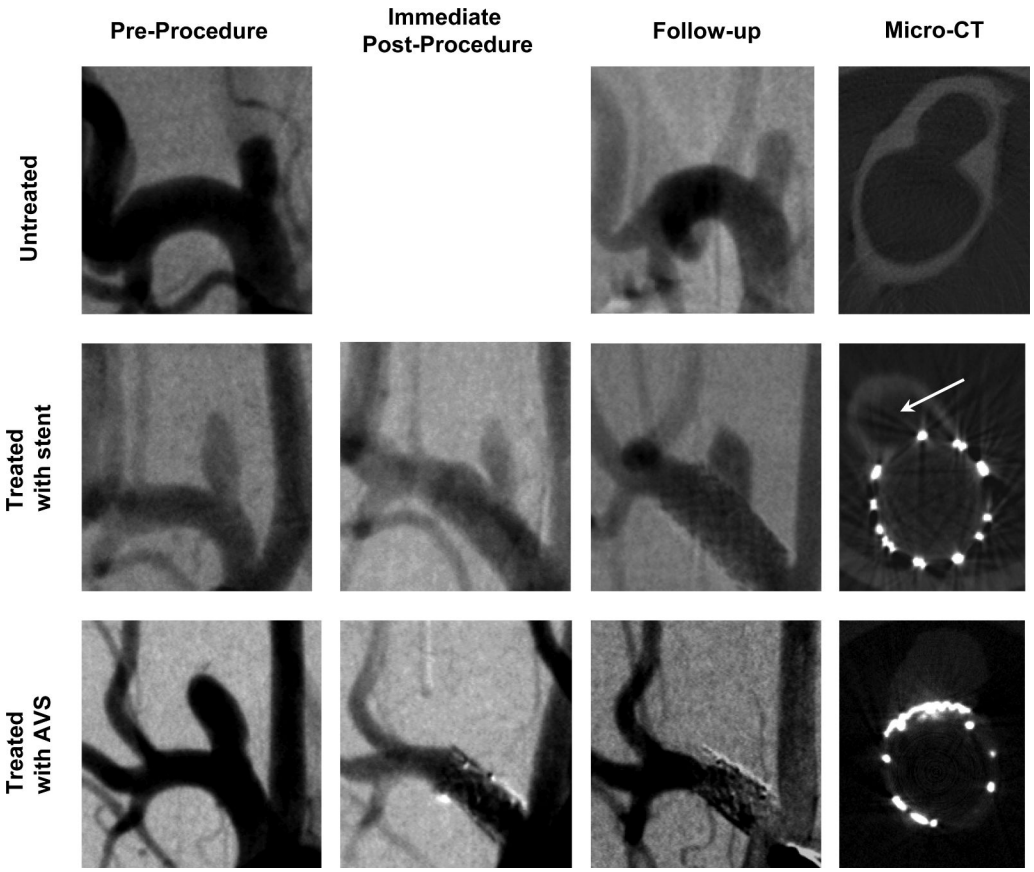

Figure 2.
Angiograms of aneurysms and Micro CT scans of the explanted aneurysms: untreated (subject #2 top row), treated with stent (subject #6 middle row) and treated with AVS (subject #11 bottom row). First three columns contain one angiographic instance: pre-procedure, immediate post-procedure and follow-up. Fourth column shows the central micro-CT slices taken perpendicular onto the aneurysm neck and parent vessel.

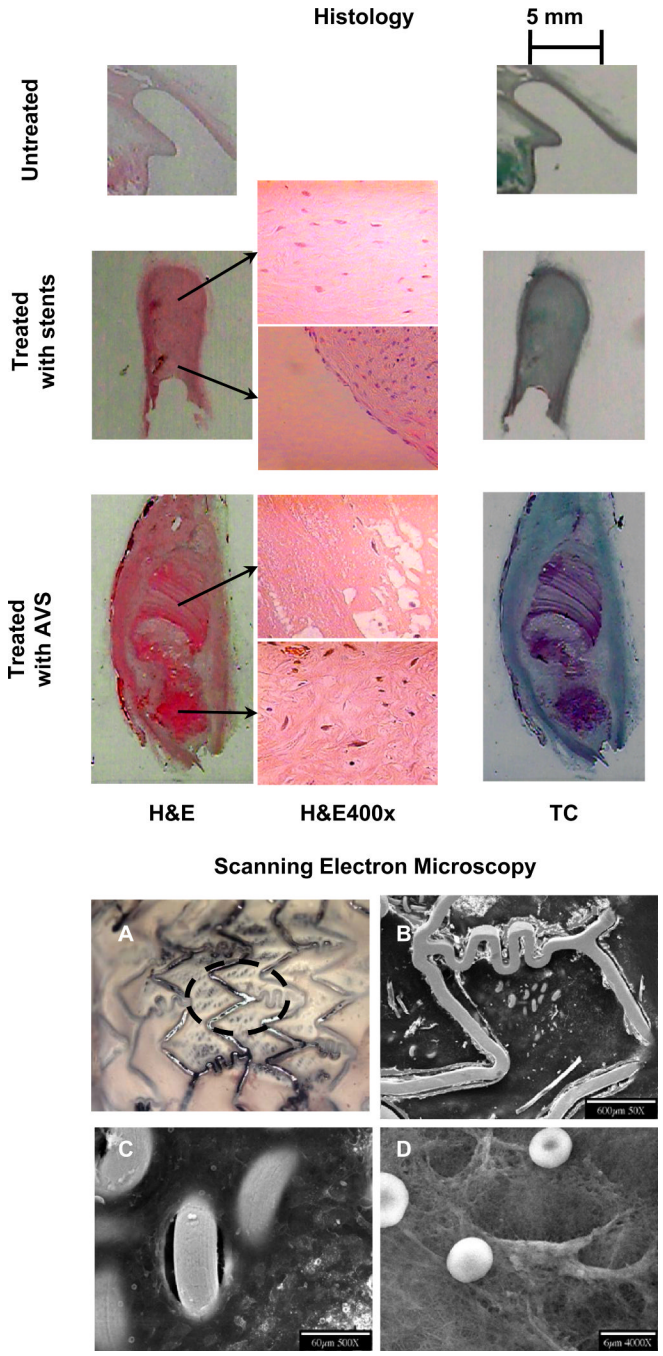

Figure 3.

Histology results: One sample from each cohort is shown in each row on the left (subjects #2 (top), #6 (middle) and #11 (bottom), respectively). Each major column shows different stains: Hematoxylin and Eosin (H&E), first column and Masson Tri-Chrome (Tc) second column. Middle column shows details taken at 400 magnification. For stent-treated aneurysms: organized thrombus in dome and remnant neck (fibroblasts in collagenous matrix) and endothelial like cells at the periphery. For AVS organized thrombus (fibroblasts, collagen, angiogenesis) are observed at the neck and “un-organized” thrombus in core of dome, mostly fibrin. SEM results (right pictures) show: (A) a low-magnification light-microscopy view of the vessel sample. The dashed circle shows the approximate position of the aneurysm neck.

(B) details of the stainless steel wires. Bare metal stent struts and partially covered fine mesh loops can be seen from the vessel lumen. (C) finer details of the vessel wall in the aneurysm neck area. Some of the mesh loops protrude directly into the vessel lumen and remain free of cellular coverage, however adjacent areas appear endothelialized. (D) regions over the patch of fine mesh appear filled with extra-cellular matrix, the presence of fresh un-deformed rbc's that are not entrapped in fibrin, suggest that the underlying extra-cellular matrix is collagenous as opposed to fibrinous.

Table 1

Summary of the Angiographic, CT and Histology results.

Group	ID	Contrast Flow			CT Scans		Histology	
		Pre-procedure	Immediate post-procedure	Follow-up	AVS placement	Aneurysms	Neck	Dome
Controls Untreated	1	*F*	*N/A*	*F*	*N/A*	*Patent*	*0*	*0*
	2	*F*		*F*		*Patent*	*0*	*2*
	3	*F*		*F*		*Patent*	*0*	*0*
	4	*F*		*F*		*Patent*	*N/A**	*N/A**
	5	*F*		*F*		*Patent*	*0*	*1*
Summary/Average Score		***100% F***	***N/A***	***100% F***		***100% Patent***	***0***	***0.75***
Treated with coronary stents	6	S^P	S^P	*F*	*N/A*	*Partially Patent*	*N/A**	*1*
	7	*F*	S^P	*F*		*Partially Patent*	*0*	*2*
	8	*F*	*F*	*F*		*patent*	*N/A**	*N/A**
	9	*F*	*O*	*O*		*Occluded*	*4*	*4*
	10	*F*	*F*	*F*		*patent*	*0*	*3*
Summary/Average Score		***80% F***	***40%S 40%F 20%O***	***80% F***		***40% P. Patent 40%Patent 20% Occluded***	***1.33***	***2.5***
Treated with AVS	11	S^P	*O*	*O*	*100%*	*Occluded*	*4*	*2*
	12	*F*	*O*	*O*	*100%*	*Occluded*	*4*	*4*
	13	*F*	*O*	*O*	*100%*	*Occluded*	*N/A**	*N/A**
	14	*F*	*O*	*O*	*100%*	*Occluded*	*4*	*3*
	15	*F*	*O*	*O*	*100%*	*Occluded*	*3*	*3*
	16	*F*	*O*	*O*	*50%*	*Occluded*	*4*	*3*
	17	*F*	*S*	*O*	*75%*	*Occluded*	*4*	*4*
	18	*F*	*O*	*O*	*>90%*	*Occluded*	*N/A**	*4*
	19	*F*	*O*	*O*	*100%*	*Occluded*	*4*	*2*
	20	*F*	*O*	*O*	*N/A*	*N/A*	*4*	*3*
Summary/Average Score		***100% F***	***90% O 10% S***	***100%O***	***66% well placed***	***100% O***	***3.4***	***3.11***

Flow classification: Pooling(P), Fast (F), Slow (S), and Occluded (O).

The histology grading scale: 0 (zero) for less than 2% thrombus; 1 (one) for 2% to 10% thrombus; 2 (two) for 10% to 50%, 3 (three) for 50% to 90% and 4 (four) if more than 90% of the area was filled with organized thrombus.

Stroke. Author manuscript; available in PMC 2010 March 1.

* **For histology some samples were excluded due to severe artifacts or defects that occurred during the processing of the aneurysms.**